

Synthesis, Characterization, and Comparative Analysis of Zinc Oxide Nanoparticles using *Calendula Officinalis* Flower Extract and its Antibacterial Activity

Logesh Radhakrishnan ¹, Samrin Abdul Sathar ¹, Shazia Jamal ¹, Santosh Kumar ²,
Neesar Ahmed ^{1,*}

¹ School of Life Sciences, B. S. Abdur Rahman Crescent Institute of Science and Technology, Vandalur, Chennai-600048, Tamil Nadu, India

² Department of Biotechnology, Guru Ghasidas Vishwavidyalaya, Bilaspur 495009, C.G., India

* Correspondence: neesar.sls@crescent.education;

Received: 30.08.2023; Accepted: 1.01.2025; Published: 5.09.2025

Abstract: Zinc oxide nanostructures have demonstrated significant reliability in the nanotechnology sector, particularly in various biomedical applications, due to their low toxicity and excellent biocompatibility, making them the most widely used metal oxide nanoparticles. This study focuses on the green synthesis of zinc oxide nanoparticles (ZnONPs) from *Calendula officinalis* flower extract as an alternative to conventional chemical methods. Comparative analysis reveals the crystalline structure of both green-synthesized and chemically synthesized ZnONPs through XRD, with chemically synthesized ZnONPs showing 2θ values of 31.64° , 34.17° , 36.12° , 47.34° , 56.57° , 62.46° , and 67.79° , while green-synthesized ZnONPs exhibit values of 31.71° , 34.52° , 36.12° , 47.68° , 56.86° , 62.86° , and 68.05° . SEM micrographs depict chemically synthesized ZnONPs as spherical and partially hexagonal, while green-synthesized ZnONPs appear spherical and bullet-shaped. EDX analysis confirms the elemental composition and purity of both types, while TEM analysis shows distinct microstructures. Notably, green-synthesized ZnONPs exhibit greater antibacterial efficacy against *Enterococcus faecalis*, *Pseudomonas aeruginosa*, and *Staphylococcus aureus*, with the highest inhibition zone noted for *Staphylococcus aureus*.

Keywords: green synthesis; *Calendula officinalis*; DRS-UV spectra; transmission electron microscopy; antibacterial activity.

© 2025 by the authors. This article is an open-access article distributed under the terms and conditions of the Creative Commons Attribution (CC BY) license (<https://creativecommons.org/licenses/by/4.0/>), which permits unrestricted use, distribution, and reproduction in any medium, provided the original work is properly cited. The authors retain copyright of their work, and no permission is required from the authors or the publisher to reuse or distribute this article, as long as proper attribution is given to the original source.

1. Introduction

Nanotechnology is defined as the development of particles with at least one measurement between 1 and 100 nanometers [1,2]. Nanoparticles have a higher surface-to-volume ratio due to their small size. In contrast to their bulk size, when particles shrink from bulk matter to nano size, their physical, chemical, and biological properties alter [3]. At this size, the different attributes of the material change, and the scientists use these features to counteract different problems in the departments of aerospace, the health sector, physics, and so on [4,5]. Nanotechnology is a rapidly developing field in industry that will revolutionize a variety of scientific fields. In the industry, a variety of metal oxide nanoparticles have been

created for various applications [6]. Nanoparticles are found to withstand high temperatures and pressure. Some of these nanomaterials, especially zinc oxide, are known to have less toxicity and also play a role in being vital to the human body [7,8]. Zinc oxide (ZnO) is one of the most influential materials employed in the industry due to its exceptional attributes, like being antibacterial and having great heat resistance [9]. Zinc oxide nanoparticles, on the other hand, are unique and have piqued scientists' curiosity due to their widespread use in a variety of sectors, due to their unique optical and chemical properties. Photocatalytic capabilities of zinc oxide (ZnO) nanoparticles have been investigated in several biological and chemical sectors for their photo-oxidizing ability [10,11]. They're also known to have antibacterial, antifungal, and UV radiation reflection and filtering properties [12]. Zinc is a mineral found in the human body that aids in metabolism and wound healing. It is crucial for eukaryotic species because it performs many of their essential physiological tasks [13]. The advancement in technology has led to the discovery of other approaches to synthesizing nanoparticles, one of which is the biological method of synthesis [14]. There are various biological sources for production, such as bacteria, fungi, and plants. Plant-interceded production of nanoparticles has been picking up a lot of attention due to the fact that it is very eco-friendly and a much more affordable method of nanoparticle synthesis compared to the other established approaches [15–17]. Also known as green synthesis, this method of producing nanoparticles by plant extracts has become a popular method in the synthesis of nanoparticles [18]. The plant used for this research is *Calendula officinalis*, also commonly known as marigold, which was originally found in the southern region of Europe. Pharmacological studies indicate that *Calendula officinalis* exhibits a wide range of biological activities, establishing it as a promising candidate for herbal-based therapies. The plant's anti-inflammatory and antioedematous properties are well-documented, alongside its antiviral activity against viruses such as influenza, HIV, and herpes simplex. *C. officinalis* essential oil also demonstrates antimicrobial efficacy, particularly against bacteria like *Bacillus subtilis* and fungi such as *Candida albicans*. Key bioactive compounds in *C. officinalis* include terpenoids (e.g., stigmaterol, sitosterol), flavonoids (e.g., quercetin, rutin), coumarins (e.g., esculetin, scopoletin), quinones, carotenoids (e.g., lycopene, lutein), volatile oils, and amino acids. These compounds collectively contribute to its medicinal properties [19]. It can reach a height of 60 cm. The flowers of this plant are usually large in size and are yellow or orange in colour. This flower have an old history in being used over many generations as remedies, creams and decoctions for sunburns and bruises in folk culture. In addition to these effects, *C. officinalis* has shown anticancer potential. Studies reveal that it induces cell cycle arrest and apoptosis in cancer cell lines, such as leukemia and colorectal cancer. The triterpenoids and triterpenes present in its methanolic extract inhibit inflammation triggered by agents like TPA and croton oil. The plant also demonstrates antiprotozoal, hepatoprotective, antioxidant, and wound-healing properties. In animal models, saponin-rich extracts of *C. officinalis* have shown antitumor efficacy. These pharmacological properties underscore the plant's therapeutic potential in various medical applications [20–22].

In this study, we report a comparative analysis of zinc oxide nanoparticles (ZnONPs) synthesized via biological and chemical methods. The biologically synthesized ZnONPs (MG-ZnONPs) were derived using *Calendula officinalis* (marigold) flower extract, while the chemically synthesized ZnONPs served as a control. Both types of ZnONPs were characterized using UV-visible diffuse reflectance spectroscopy (DRS-UV), Fourier transform infrared spectroscopy (FTIR), X-ray diffraction (XRD), transmission electron microscopy (TEM), scanning electron microscopy (SEM), and energy dispersive X-ray spectroscopy (EDX). The

antibacterial efficiency of biosynthesized ZnONPs was assessed and compared with their chemically synthesized counterparts, highlighting the potential advantages of green synthesis for antibacterial applications.

2. Materials and Methods

2.1. Materials.

The chemicals used in this work are analytical grade, 99% pure. Molecular biology grade zinc nitrate [$\text{Zn}(\text{NO}_3)_2$] was purchased from SRL, India. *Calendula officinalis* (marigold) flowers were purchased from the nearby market of BSA Crescent Institute of Science and Technology, Vandalur, Chennai. Double-distilled water was used for reagent preparation in the overall experiment.

2.2. Preparation of flower extract and preliminary phytochemical analysis.

Calendula officinalis (marigold) flower petals were washed with double-distilled water thrice, followed by being baked under the shade of the sun, and were also left to dry in a hot air oven at 60°C for 6 hours. Then, the dried flower petals were ground into fine particles using a mortar and pestle. 10 g of grain powder was taken and put in 100 mL of double-distilled water, and the mixture was boiled with continuous stirring at 60°C for 20 to 30 minutes. The solution mixture was drained through a muslin cloth to get the flower extract [15]. After the preparation of the flower extract, the preliminary phytochemical analysis was done using an already existing protocol [23,24].

2.3. Synthesis of ZnONPs using the co-precipitation method.

ZnONPs are chemically synthesized using the co-precipitation method. In the 0.2 M zinc nitrate solution, 0.5 M NaOH was added drop-wise, stirring at room temperature for 3 to 5 hours. After that, the precipitate was centrifuged, the supernatant was discarded, and the pellet was washed with distilled water twice. After washing, the purified ZnONPs were dried in a hot air oven overnight at 60°C [25–27].

2.4. Biosynthesis and purification of ZnONPs using *Calendula officinalis* (marigold) flower extract.

In 25 mL of 0.2 M zinc nitrate solution, 5 mL of *Calendula officinalis* (marigold) flower extract was added, then the mixture was mixed for 2.5 hours using a magnetic mixer. 0.5 NaOH was added drop-wise, stirring at room temperature for 3 to 5 hours. After that, the precipitate was centrifuged, the supernatant was discarded, and the pellet was washed with distilled water twice. After washing, the purified MG-ZnONPs were dried in a hot air oven overnight at 60°C.

2.5. Characterization of synthesized ZnONPs.

The dried ZnONPs were crushed into fine powder using a mortar and pestle and subjected to characterization using different analyses. The optical properties of the ZnONPs were studied using UV-Vis diffuse reflectance spectra (DRS-UV), and spectra were taken in the wavelength range from 200 to 1400 nm at room temperature on a UV 2600 (Shimadzu) model spectroscopy. The functional groups of the ZnONPs and the spectral properties were analyzed using FT-IR (Fourier transform infrared spectroscopy) analysis. The samples were

read at a spectral range between $400\text{-}4000\text{cm}^{-1}$ with 4 cm^{-1} resolution at room temperature using the spectroscopy model JASCO FTIR-6300 (Massachusetts, USA). The crystalline nature of the synthesized ZnONPs was examined using an X-ray diffractometer (XRD) with the X'pert powder XRD system under Cu $K\alpha$ radiation ($\lambda=1.5406\text{ \AA}$), vertical goniometer type. Microscopic analysis was examined using SEM and TEM analysis to observe the structural morphology of the synthesized ZnONPs by SEM (FEI-QUANTA-FEG 200), which was operated at an acceleration voltage range of $200\text{ V} - 30\text{ kV}$, and TEM was carried out by JEOL-JEM 2100 operated at an acceleration voltage of 200 kV . The Energy dispersive spectrum was also examined for both chemically and green synthesized ZnONPs to ensure the elemental composition.

2.6. Analysis of antibacterial activity.

Antibacterial activity was done for both chemically and green synthesized ZnONPs against harmful and infectious bacteria *Enterococcus faecalis*, *Pseudomonas aeruginosa*, and *Staphylococcus aureus*. A good diffusion method was used to compare the antibacterial activity of the ZnONPs. $100\text{ }\mu\text{g/mL}$ of both samples was added to the wells and incubated at 37°C . After overnight incubation, the zone of inhibition (size) was measured, and the experiment was done in triplicate.

3. Results and Discussion

3.1. UV-Vis diffuse reflectance spectra (DRS-UV).

Figures 1a and b depict the ultraviolet-visible diffuse reflection spectra (UV-Vis DRS) absorption of the chemically and green synthesized ZnONPs. The adsorption range of both ZnONPs was absorbed at a wavelength range between $(200\text{-}400\text{ nm})$, and the absorption peak of the green synthesized ZnONPs (Figure 1a) slightly differed compared to the chemically synthesized ZnONPs absorption (Figure 1b). Both nanoparticles have a great amount of absorption in the UV zone, and the absorption band intensity was also noted in the production of ZnONPs in both methods. High absorbance was measured at a range of 385 nm in green synthesized ZnONPs (Figure 1a), but in chemically synthesized ZnONPs, the UV-Vis DRS absorbance range was near 390 nm (Figure 1b). The previous reports also show that the ZnONPs absorbance range is equal to our finding. Higher extract concentrations typically result in nanoparticles with enhanced optical properties, such as a blue shift in UV-vis absorption spectra, which occurs due to the quantum confinement effect in smaller particles [28,29].

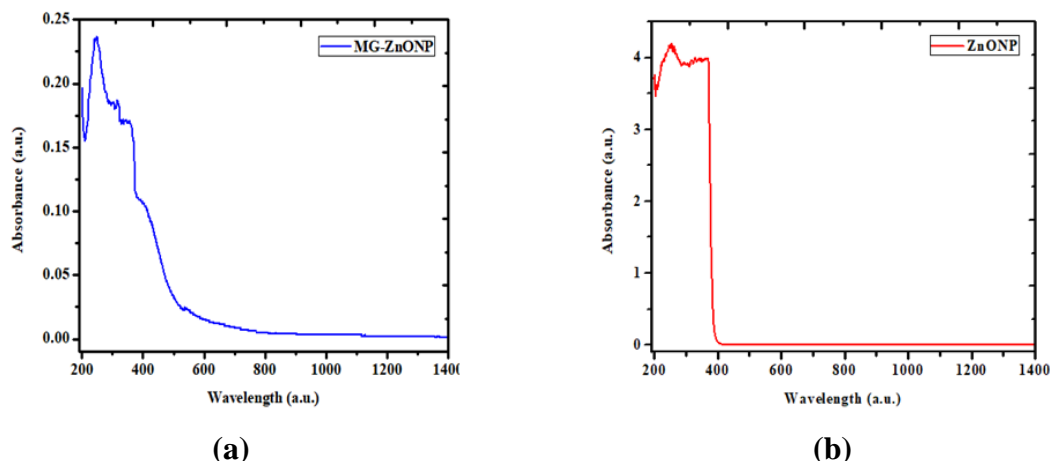


Figure 1. UV-DRS spectrum analysis of (a) MG-ZnONPs; (b) ZnONPs.

3.2. Fourier transform infrared spectroscopy (FT-IR).

The FTIR characterization was done for both chemically and green-synthesized ZnONPs (Figures 2a and b). The broad peak at 3362.28 cm^{-1} (Figure 2a) in MG-ZnONPs (Green synthesized ZnONPs using *Calendula officinalis* (marigold) flower extract) and 3429.78 cm^{-1} (Figure 2b) in chemically synthesized ZnONPs denotes that O-H stretching. The weak peak at 2925.48 cm^{-1} in MG-ZnONPs indicates the CH_3 stretching vibration (Figure 2a). Medium peaks at 1588.09 cm^{-1} in MG-ZnONPs and 1644.02 cm^{-1} in ZnONPs represent the N-H bending presence of the amine group (Figures 2a and b). Medium peaks at 1413.57 cm^{-1} in MG-ZnONPs and 1363.78 cm^{-1} in ZnONPs represent the O-H bending. The peak at 487.902 cm^{-1} in MG-ZnONPs and 520.686 cm^{-1} in ZnONPs confirms the presence of Zn-O stretching. Usually, metal oxide peaks are between $600\text{--}400\text{ cm}^{-1}$ [10]. The broad peaks at 3362.28 cm^{-1} in the green synthesized ZnONPs indicate the presence of phenol phytochemicals, and this phenol helps in the reduction and stabilization of the nanoparticles. In the same way, a peak at 400 to 600 cm^{-1} confirms the presence of ZnONPs [30–32].

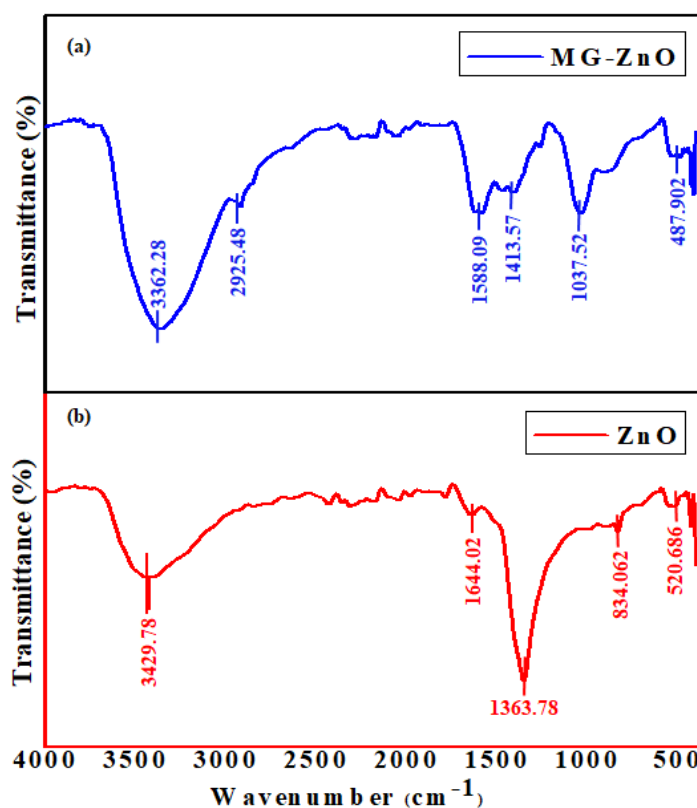


Figure 2. FTIR analysis of (a) MG-ZnONPs; (b) ZnONPs.

3.3. X-ray diffraction analysis (XRD).

XRD helps in indicating the crystalline structure of both chemically and green synthesized ZnONPs (Figures 3a and b). Figure 3(a and b) shows the spectrum of X-ray diffraction caused by both ZnONPs. Crucial diffraction peaks observed here correlate with the Bragg reflections with 2θ values of chemically synthesized ZnONPs (Figure 3a) 31.64° , 34.17° , 36.12° , 47.34° , 56.57° , 62.46° , and 67.79° . 2θ values of green synthesized (MG-ZnONPs) are 31.71° , 34.52° , 36.12° , 47.68° , 56.86° , 62.86° and 68.05° in (Figure 3b). Locations of the distinct peaks were indexed to (100), (002), (101), (102), (110), (103), and (112) planes of the diffraction lattice, respectively [33]. The 2θ values of both ZnONPs are similarly matching with earlier reports [34–36].

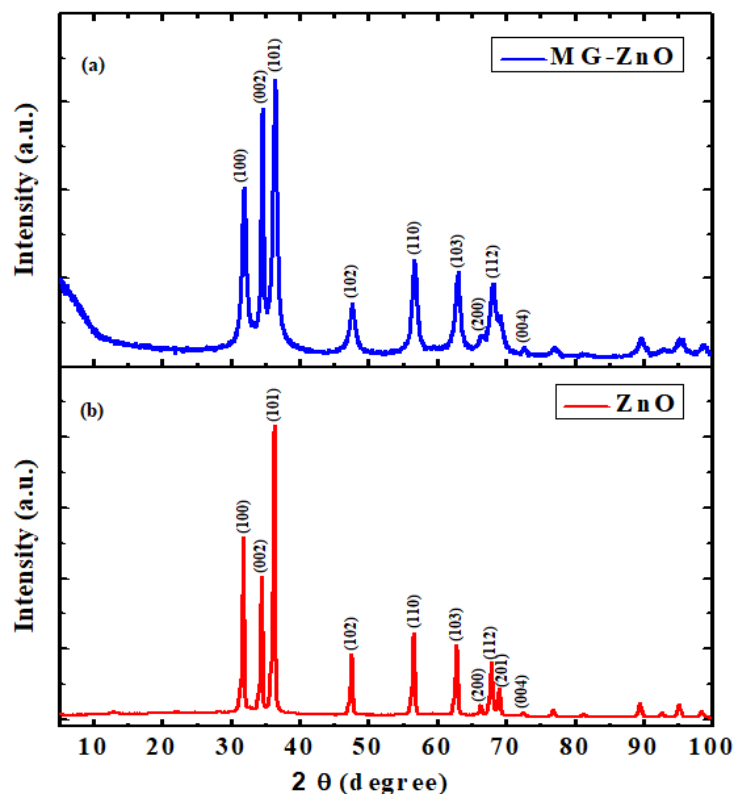


Figure 3. XRD analysis of (a) MG-ZnONPs; (b) ZnONPs.

3.4. SEM and EDX analysis.

The shape and structure of the synthesized ZnONPs were examined by SEM and EDX analysis (Figures 4 and 5). The SEM micrograph of the chemically synthesized ZnONPs reveals that particles are in spherical, partially hexagonal, and accumulation form (Figure 4a). The green synthesized ZnONPs SEM micrograph reveals that biologically synthesized Zinc oxide particles are spherical, aggregate, and accumulate in a bullet shape (Figure 4b).

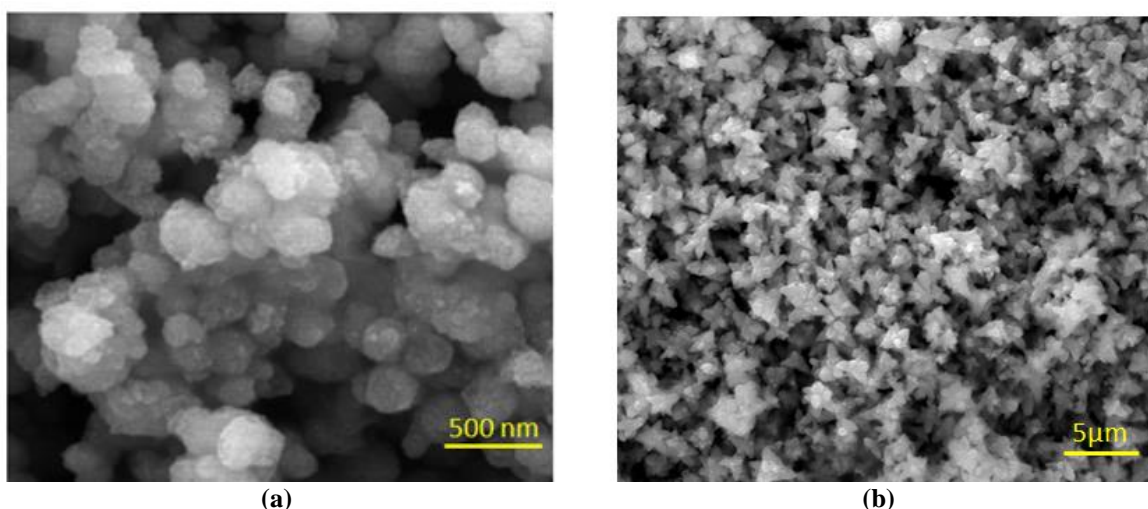
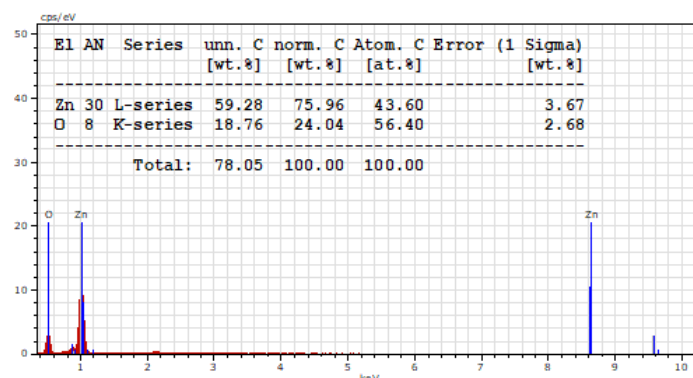
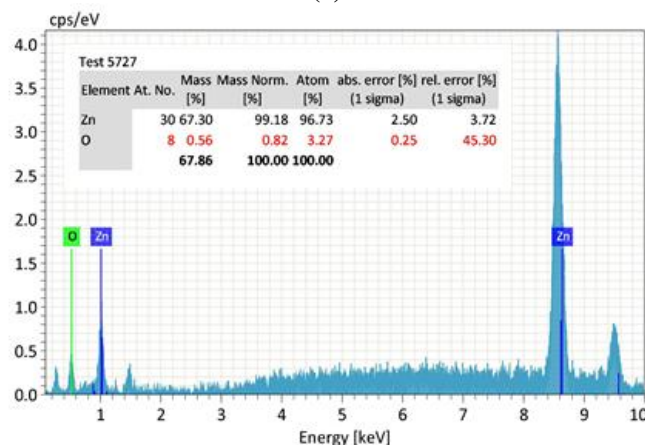


Figure 4. Morphological analysis-FESEM images. (a) ZnONPs; (b) MG-ZnONPs.

The EDX plot of both chemically and biologically synthesized ZnONPs revealed the elemental composition of the nanoparticles (Figure 5a and b). This EDX plot shows the purity of the nanoparticles and the Zn and Oxygen element composition of both ZnONPs (Figure 5a and b).



(a)

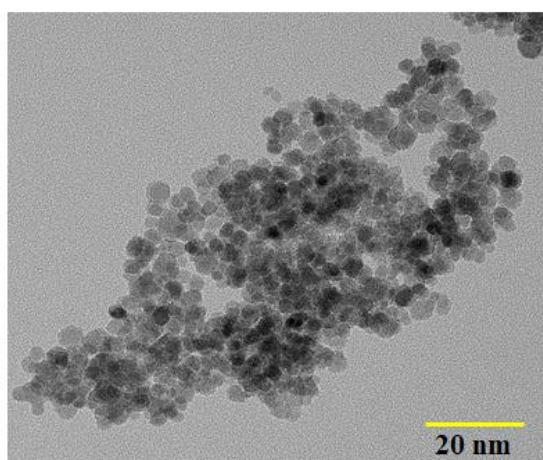


(b)

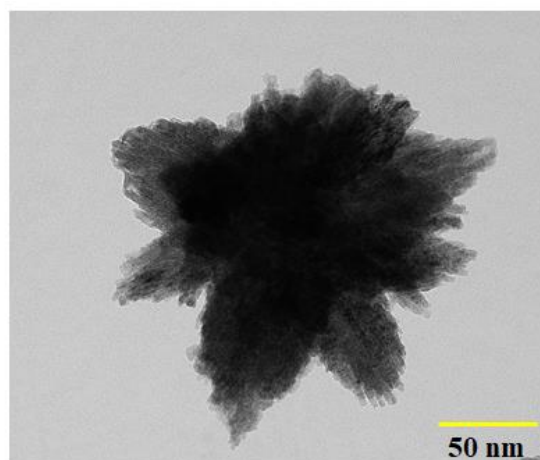
Figure 5. EDX spectrum analysis. (a) ZnONPs; (b) MG-ZnONPs.

3.5. TEM analysis.

The microstructure and shape of the synthesized ZnONPs are examined using TEM analysis, and the morphologies of the chemically and green synthesized ZnONPs taken from high-resolution TEM analysis are shown in Figures 6a and b. Chemically synthesized ZnONPs are hexagonal and spherical in shape in the accumulation (Figure 6a). The microstructure of the green synthesized ZnONPs is revealed in HRTEM analysis, and MG-ZnONPs are in spherical and aggregated bullet-shaped nanoparticles (Figure 6b).



(a)



(b)

Figure 6. Morphological analysis-HRTEM images. (a) ZnONPs; (b) MG-ZnONPs.

The synthesis of zinc oxide nanoparticles (ZnONPs) using *Calendula officinalis* extract, a green and eco-friendly method, is significantly influenced by the concentration of the plant extract. This concentration plays a vital role in determining the size, shape, and properties of the ZnONPs produced. At lower concentrations of *Calendula officinalis* extract, fewer phytochemicals (e.g., flavonoids, terpenoids, and phenolic compounds) are available to reduce zinc ions, leading to slower nucleation rates and the formation of larger nanoparticles. Larger particle sizes are often a result of prolonged growth phases, as fewer nuclei are formed initially. On the other hand, higher concentrations of the extract increased the availability of reducing and capping agents, which facilitates faster nucleation and restricts nanoparticle growth, resulting in smaller ZnONPs. The concentration of the extract also influences the shape of the synthesized ZnONPs. Higher concentrations of *Calendula officinalis* provide more capping molecules, leading to more controlled anisotropic growth, which can produce well-defined shapes such as spherical, hexagonal, or rod-like structures. In contrast, lower concentrations may result in irregularly shaped nanoparticles due to insufficient capping agents to regulate growth patterns.

3.6. Antibacterial activity.

The antibacterial activity of the ZnONPs is based on the nanoparticle's shape and morphology. Higher concentrations enhance the antibacterial, antioxidant, and photocatalytic activities of ZnONPs, as smaller particles with larger surface areas exhibit better interaction with microbial cells and catalytic systems. In this study, we have done an antibacterial study against three different bacteria (*Enterococcus faecalis*, *Pseudomonas aeruginosa*, and *Staphylococcus aureus*) using synthesized nanoparticles (ZnONPs and MG-ZnONPs). Compared to chemically synthesized ZnONPs, green-synthesized ZnONPs are more effective for the above-mentioned bacterial species. The zone of inhibition (size in mm) of each bacterium is mentioned in Table 1. Between these three bacterial species in both ZnONPs, compared to *Enterococcus faecalis* (Figure 7a) and *Pseudomonas aeruginosa* (Figure 7b), in *Staphylococcus aureus* culture plate (Figure 7c), the zone of inhibition (size in mm) was high (Table 1).

Table 1. Zone of Inhibition (in mm).

Sample (100µg/ml)	<i>Enterococcus faecalis</i>	<i>Pseudomonas aeruginosa</i>	<i>Staphylococcus aureus</i>
MG-ZnONPs	8.0 mm	14.0 mm	15.0 mm
ZnONPs	7.2 mm	11.5 mm	13.0 mm

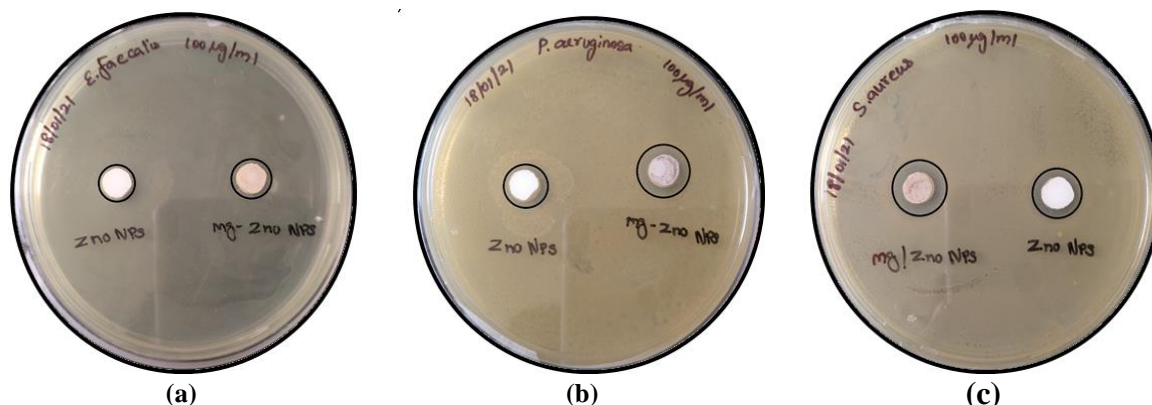


Figure 7. Antibacterial activity of ZnO and MG-ZnO nanoparticles (a) *Enterococcus faecalis*; (b) *Pseudomonas aeruginosa*; (c) *Staphylococcus aureus*.

Biosynthesized zinc oxide nanoparticles (ZnONPs) exhibit superior antibacterial activity compared to their chemically synthesized counterparts, largely due to the presence of capping agents derived from plant extracts. These agents provide additional functional groups that enhance the nanoparticles' surface charge and chemical interactions, promoting better adhesion to bacterial cell walls and facilitating disruption of bacterial membranes. Moreover, these capping agents aid in generating reactive oxygen species (ROS), further enhancing bacterial inhibition. The combined effects of particle size, surface charge, and bioactive capping agents make biosynthesized ZnONPs highly effective for antimicrobial applications [13,25].

4. Conclusions

In this study, we synthesized zinc oxide nanoparticles both chemically and biologically, and a synthesis of ZnONPs using *Calendula officinalis* (marigold) flower extract was done. The use of *Calendula officinalis* extract in the green synthesis of zinc oxide nanoparticles (ZnONPs) significantly impacts their size, shape, and functional properties. Optimizing the concentration of this extract is crucial for tailoring ZnONPs for various applications, such as in medicine and environmental remediation. Green-synthesized ZnONPs demonstrate superior thermal stability, with studies showing a weight loss of only about 29% when heated to 1000°C, primarily due to moisture and organic compound loss, without major structural degradation. Furthermore, phenolic compounds in the plant extract act as natural stabilizers, enhancing the nanoparticles' resistance to oxidation and environmental stress, which chemically synthesized ZnONPs lack. These bioactive compounds also protect ZnONPs from environmental factors like high temperatures and pH variations. Green synthesis thus provides a more environmentally friendly and sustainable approach compared to conventional chemical methods. DRS-Uv spectra, FTIR, and XRD results of synthesized products confirm the presence of ZnONPs. Morphological studies like SEM, EDX, and TEM results revealed that synthesized nanoparticles are spherical in shape, and interestingly, green synthesized ZnONPs accumulate and look like bullets in shape. The EDX plot of both nanoparticles confirms the purity of the product and the composition of Zn and oxygen. Antibacterial activity against three different bacteria (*Enterococcus faecalis*, *Pseudomonas aeruginosa*, and *Staphylococcus aureus*) confirms the biological properties of the nanoparticles. Interestingly, in antibacterial activity, compared to chemically synthesized ZnONPs, green synthesized ZnONPs have more bacterial growth inhibition properties. The conclusion of this study is that our findings will be more eco-friendly and an alternative to the recent biological compounds used to treat bacterial infections.

Author Contributions

Conceptualization, N.A. and S.J.; methodology, L.R. and S.A.S.; formal analysis, L.R., S.A.S., N.A.; writing—original draft preparation, L.R. and S.A.S.; writing—review and editing- N.A., S.J., S.K.; supervision, N.A. and S.J.; project administration, N.A.; funding acquisition, L.R. All authors have read and agreed to the published version of the manuscript.

Institutional Review Board Statement

Not applicable.

Informed Consent Statement

Not applicable.

Data Availability Statement

Data supporting the findings of this study are available upon reasonable request from the corresponding author.

Funding

L.R. received ICMR SRF: 2020-0056/CMB-BMS.

Acknowledgments

We would like to acknowledge the support provided by the Department of Chemistry for FTIR.

Conflicts of Interest

The authors declare no conflict of interest.

Reference

1. Abel, S.; Tesfaye, J.L.; Shanmugam, R.; Dwarampudi, L.P.; Lamessa, G.; Nagaprasad, N.; Benti, M.; Krishnaraj, R. Green Synthesis and Characterizations of Zinc Oxide (ZnO) Nanoparticles Using Aqueous Leaf Extracts of Coffee (*Coffea Arabica*) and Its Application in Environmental Toxicity Reduction. *Journal of Nanomaterials* **2021**, *2021*, e3413350, <https://doi.org/10.1155/2021/3413350>.
2. Gur, T.; Meydan, I.; Seckin, H.; Bekmezci, M.; Sen, F. Green Synthesis, Characterization and Bioactivity of Biogenic Zinc Oxide Nanoparticles. *Environ. Res.* **2022**, *204*, 111897, <https://doi.org/10.1016/j.envres.2021.111897>.
3. Pirtarighat, S.; Ghannadnia, M.; Baghshahi, S. Green Synthesis of Silver Nanoparticles Using the Plant Extract of *Salvia Spinosa* Grown in Vitro and Their Antibacterial Activity Assessment. *J. Nanostruct. Chem.* **2019**, *9*, 1–9, <https://doi.org/10.1007/s40097-018-0291-4>.
4. Saini, R.; Saini, S.; Sharma, S. Nanotechnology: The Future Medicine. *J. Cutan. Aesthet. Surg.* **2010**, *3*, 32–33, <https://doi.org/10.4103/0974-2077.63301>.
5. Chandhru, M.; Logesh, R.; Kutti Rani, S.; Ahmed, N.; Vasimalai, N. Green Synthesis of Silver Nanoparticles from Plant Latex and Their Antibacterial and Photocatalytic Studies. *Environ. Technol.* **2022**, *43*, 3064–3074, <https://doi.org/10.1080/09593330.2021.1914181>.
6. Xu, J.; Huang, Y.; Zhu, S.; Abbes, N.; Jing, X.; Zhang, L. A Review of the Green Synthesis of ZnO Nanoparticles Using Plant Extracts and Their Prospects for Application in Antibacterial Textiles. *Journal of Engineered Fibers and Fabrics* **2021**, *16*, 15589250211046242, <https://doi.org/10.1177/15589250211046242>.
7. Kahsay, M.H. Synthesis and Characterization of ZnO Nanoparticles Using Aqueous Extract of *Becium Grandiflorum* for Antimicrobial Activity and Adsorption of Methylene Blue. *Appl. Water Sci.* **2021**, *11*, 45, <https://doi.org/10.1007/s13201-021-01373-w>.
8. Vijayakumar, N.; Bhuvaneshwari, V.K.; Ayyadurai, G.K.; Jayaprakash, R.; Gopinath, K.; Nicoletti, M.; Alarifi, S.; Govindarajan, M. Green Synthesis of Zinc Oxide Nanoparticles Using *Anoectochilus Elatus*, and Their Biomedical Applications. *Saudi. J. Biol. Sci.* **2022**, *29*, 2270–2279, <https://doi.org/10.1016/j.sjbs.2021.11.065>.
9. Hasnidawani, J.N.; Azlina, H.N.; Norita, H.; Bonnia, N.N.; Ratim, S.; Ali, E.S. Synthesis of ZnO Nanostructures Using Sol-Gel Method. *Procedia Chemistry* **2016**, *19*, 211–216, <https://doi.org/10.1016/j.proche.2016.03.095>.
10. Fakhari, S.; Jamzad, M.; Kabiri Fard, H. Green Synthesis of Zinc Oxide Nanoparticles: A Comparison. *Green Chemistry Letters and Reviews* **2019**, *12*, 19–24, <https://doi.org/10.1080/17518253.2018.1547925>.

11. Abel, S.; Tesfaye, J.L.; Nagaprasad, N.; Shanmugam, R.; Dwarampudi, L.P.; Krishnaraj, R. Synthesis and Characterization of Zinc Oxide Nanoparticles Using Moringa Leaf Extract. *Journal of Nanomaterials* **2021**, *2021*, e4525770, <https://doi.org/10.1155/2021/4525770>.
12. Ashwini, J.; Aswathy, T.R.; Rahul, A.B.; Thara, G.M.; Nair, A.S. Synthesis and Characterization of Zinc Oxide Nanoparticles Using Acacia Caesia Bark Extract and Its Photocatalytic and Antimicrobial Activities. *Catalysts* **2021**, *11*, 1507, <https://doi.org/10.3390/catal11121507>.
13. Siddiqi, K.S.; ur Rahman, A.; Tajuddin; Husen, A. Properties of Zinc Oxide Nanoparticles and Their Activity Against Microbes. *Nanoscale Res. Lett.* **2018**, *13*, 141, <https://doi.org/10.1186/s11671-018-2532-3>.
14. Faisal, S.; Jan, H.; Shah, S.A.; Shah, S.; Khan, A.; Akbar, M.T.; Rizwan, M.; Jan, F.; Wajidullah; Akhtar, N.; Khattak, A.; Syed, S. Green Synthesis of Zinc Oxide (ZnO) Nanoparticles Using Aqueous Fruit Extracts of Myristica Fragrans: Their Characterizations and Biological and Environmental Applications. *ACS Omega* **2021**, *6*, 9709–9722, <https://doi.org/10.1021/acsomega.1c00310>.
15. Aritonang, H.F.; Koleangan, H.; Wuntu, A.D. Synthesis of Silver Nanoparticles Using Aqueous Extract of Medicinal Plants' (Impatiens Balsamina and Lantana Camara) Fresh Leaves and Analysis of Antimicrobial Activity. *Int. J. Microbiol.* **2019**, *2019*, 8642303, <https://doi.org/10.1155/2019/8642303>.
16. Chandhru, M.; Logesh, R.; Rani, S.K.; Ahmed, N.; Vasimalai, N. One-Pot Green Route Synthesis of Silver Nanoparticles from Jack Fruit Seeds and Their Antibacterial Activities with Escherichia Coli and Salmonella Bacteria. *Biocatalysis and Agricultural Biotechnology* **2019**, *20*, 101241, <https://doi.org/10.1016/j.bcab.2019.101241>.
17. Jayachandran, A.; T.r.A.; Nair, A.S. Green Synthesis and Characterization of Zinc Oxide Nanoparticles Using Cayratia Pedata Leaf Extract. *Biochemistry and Biophysics Reports* **2021**, *26*, 100995, <https://doi.org/10.1016/j.bbrep.2021.100995>.
18. M, N.; R, S. Green Synthesis Of Silver Nanoparticles Using *Calendula Officinalis* And Its Anti-Bacterial Studies. *Mapana Journal of Sciences* **2018**, *17*, 11–17, <https://doi.org/10.12723/mjs.45.2>.
19. Shahane, K.; Kshirsagar, M.; Tambe, S.; Jain, D.; Rout, S.; Ferreira, M.K.M.; Mali, S.; Amin, P.; Srivastav, P.P.; Cruz, J.; Lima, R.R. An Updated Review on the Multifaceted Therapeutic Potential of *Calendula Officinalis* L. *Pharmaceutical* **2023**, *16*, 611, <https://doi.org/10.3390/ph16040611>.
20. Tabassum, N.; Hamdani, M. Plants Used to Treat Skin Diseases. *Pharmacogn Rev* **2014**, *8*, 52–60, <https://doi.org/10.4103/0973-7847.125531>.
21. Siddiquee, S.; McGee, M.A.; Vincent, A.D.; Giles, E.; Clothier, R.; Carruthers, S.; Penniment, M. Efficacy of Topical *Calendula Officinalis* on Prevalence of Radiation-Induced Dermatitis: A Randomised Controlled Trial. *Australas J. Dermatol.* **2021**, *62*, e35–e40, <https://doi.org/10.1111/ajd.13434>.
22. Kadowaki, W.; Miyata, R.; Fujinami, M.; Sato, Y.; Kumazawa, S. Catechol-O-Methyltransferase Inhibitors from *Calendula Officinalis* Leaf. *Molecules* **2023**, *28*, 1333, <https://doi.org/10.3390/molecules28031333>.
23. Afzal, T.; Bibi, Y.; Ishaque, M.; Masood, S.; Qayyum, A.; Nisa, S.; Shah, Z.H.; Alsamadany, H.; Chung, G. Pharmacological Properties and Preliminary Phytochemical Analysis of Pseudocaryopteris Foetida (D.Don) P.D. Cantino Leaves. *Saudi J. Biol. Sci.* **2022**, *29*, 1185–1190, <https://doi.org/10.1016/j.sjbs.2021.09.048>.
24. Nakaziba, R.; Lubega, A.; Ogwal-Okeng, J.; Alele, P.E. Phytochemical Analysis, Acute Toxicity, as Well as Antihyperglycemic and Antidiabetic Activities of Corchorus Olitorius L. Leaf Extracts. *ScientificWorldJournal* **2022**, *2022*, 1376817, <https://doi.org/10.1155/2022/1376817>.
25. Nithya, K.; Kalyanasundharam, S. Effect of Chemically Synthesis Compared to Biosynthesized ZnO Nanoparticles Using Aqueous Extract of C. Halicacabum and Their Antibacterial Activity. *OpenNano* **2019**, *4*, 100024, <https://doi.org/10.1016/j.onano.2018.10.001>.
26. Ikram, Dr.M.; Iqbal, A.; Shaheen, S.; Haider, A.; Haider, J.; Ul-Hamid, A.; Nabgan, W.; Imran, M.; Shahzadi, A. Graphene Oxide-ZnO Nanorods for Efficient Dye Degradation, Antibacterial and In-Silico Analysis. *Applied Nanoscience* **2022**, *12*, 165-177, <https://doi.org/10.1007/s13204-021-02251-2>.
27. Vignesh, K.; Nair, A.; Chinnathambi, U.; Kalaivani, T. Synthesis and Characterization ZnO Nanoparticles Using Sol-Gel Method and Their Antibacterial Study. *IOP Conference Series: Materials Science and Engineering* **2022**, *1219*, 012019, <https://doi.org/10.1088/1757-899X/1219/1/012019>.
28. Khan, M.M.; Saadah, N.; Khan, M.; Harunsani, M.; Tan, A.; Cho, M.H. Phytogenic Synthesis of Band Gap-Narrowed ZnO Nanoparticles Using the Bulb Extract of Costus Woodsonii. *BioNanoScience* **2019**, *9*, <https://doi.org/10.1007/s12668-019-00616-0>.
29. Nhu, V.T.T.; Dat, N.D.; Tam, L.-M.; Phuong, N.H. Green Synthesis of Zinc Oxide Nanoparticles toward Highly Efficient Photocatalysis and Antibacterial Application. *Beilstein J. Nanotechnol.* **2022**, *13*, 1108–1119, <https://doi.org/10.3762/bjnano.13.94>.

30. Tiwari, A.K.; Jha, S.; Singh, A.K.; Mishra, S.K.; Pathak, A.K.; Ojha, R.P.; Yadav, R.S.; Dikshit, A. Innovative Investigation of Zinc Oxide Nanoparticles Used in Dentistry. *Crystals* **2022**, *12*, 1063, <https://doi.org/10.3390/cryst12081063>.
31. Khan, A.U.; Malik, N.; Singh, B.; Ansari, N.H.; Rehman, M.; Yadav, A. Biosynthesis, and Characterization of Zinc Oxide Nanoparticles (ZnONPs) Obtained from the Extract of Waste of Strawberry. *J.Umm Al-Qura Univ. Appl. Sci.* **2023**, *9*, 268-275, <https://doi.org/10.1007/s43994-023-00038-5>.
32. Elhamdi, I.; Souissi, H.; Taktak, O.; Elghoul, J.; Kammoun, S.; Dhahri, E.; Costa, B.F.O. Experimental and Modeling Study of ZnO:Ni Nanoparticles for near-Infrared Light Emitting Diodes. *RSC Adv.* **2022**, *12*, 13074–13086, <https://doi.org/10.1039/d2ra00452f>.
33. Lyimo, G.V.; Ajayi, R.F.; Maboza, E.; Adam, R.Z. A Green Synthesis of Zinc Oxide Nanoparticles Using Musa Paradisiaca and Rooibos Extracts. *MethodsX* **2022**, *9*, 101892, <https://doi.org/10.1016/j.mex.2022.101892>.
34. Albarakaty, F.M.; Alzaban, M.I.; Alharbi, N.K.; Bagrwan, F.S.; Abd El-Aziz, A.R.M.; Mahmoud, M.A. Zinc Oxide Nanoparticles, Biosynthesis, Characterization and Their Potent Photocatalytic Degradation, and Antioxidant Activities. *Journal of King Saud University - Science* **2023**, *35*, 102434, <https://doi.org/10.1016/j.jksus.2022.102434>.
35. Haghighat, M.; Alijani, H.Q.; Ghasemi, M.; Khosravi, S.; Borhani, F.; Sharifi, F.; Iravani, S.; Najafi, K.; Khatami, M. Cytotoxicity Properties of Plant-Mediated Synthesized K-Doped ZnO Nanostructures. *Bioprocess Biosyst. Eng.* **2022**, *45*, 97–105, <https://doi.org/10.1007/s00449-021-02643-2>.
36. Wang, Q.; Mei, S.; Manivel, P.; Ma, H.; Chen, X. Zinc Oxide Nanoparticles Synthesized Using Coffee Leaf Extract Assisted with Ultrasound as Nanocarriers for Mangiferin. *Current Research in Food Science* **2022**, *5*, 868–877, <https://doi.org/10.1016/j.crfs.2022.05.002>.

Publisher's Note & Disclaimer

The statements, opinions, and data presented in this publication are solely those of the individual author(s) and contributor(s) and do not necessarily reflect the views of the publisher and/or the editor(s). The publisher and/or the editor(s) disclaim any responsibility for the accuracy, completeness, or reliability of the content. Neither the publisher nor the editor(s) assume any legal liability for any errors, omissions, or consequences arising from the use of the information presented in this publication. Furthermore, the publisher and/or the editor(s) disclaim any liability for any injury, damage, or loss to persons or property that may result from the use of any ideas, methods, instructions, or products mentioned in the content. Readers are encouraged to independently verify any information before relying on it, and the publisher assumes no responsibility for any consequences arising from the use of materials contained in this publication.